IEEE Access
Multidisciplinary | Rapid Review | Open Access Journal

Received 3 November 2023, accepted 13 November 2023, date of publication 21 November 2023,
date of current version 29 November 2023.

Digital Object Identifier 10.1109/ACCESS.2023.3335379

APPLIED RESEARCH

Improving the Estimation of a Sucker Rod Pumping Dynamometer Card Based on the Terminal Quantities of the Driving Motor

LÁZARO EDMILSON BRITO SILVA[1], JÉS JESUS FIAIS CERQUEIRA[2], (Member, IEEE), AMAURI OLIVEIRA[2], (Life Senior Member, IEEE), AND ANTONIO MARCUS N. LIMA[3], (Senior Member, IEEE)

[1]Federal Institute of Education, Science, and Technology of Bahia, Santo Amaro 44200-000, Brazil
[2]Department of Electrical and Computer Engineering, Universidade Federal da Bahia, Salvador 41210-630, Brazil
[3]Department of Electrical Engineering, Universidade Federal de Campina Grande, Campina Grande 58429-900, Brazil

Corresponding author: Lázaro Edmilson Brito Silva (lazaro.brito@uol.com.br)

This work was supported in part by the Coordination of Improvement of Higher Education Professionals of Brazil (CAPES)-Finance Code 001.

ABSTRACT Rod pumping systems typically require the analysis of dynamometer cards for fault diagnosis. While external instrumentation assists in obtaining these cards, it simultaneously raises monitoring costs and complexity. To address this issue, this paper introduces a parameter estimator that integrates the equivalent circuit model of an induction motor with the beam pumping unit model. We have compared the performance of two practical estimators, utilizing the terminal quantities of the driving motor as inputs. The results demonstrate surface dynamometer cards under varying operational conditions of the oil well. By augmenting the estimator's input variables, the estimated cards align more closely with the actual ones. This practical application proposes an alternative method for acquiring the surface dynamometer card, which can function as a supplementary approach in fault diagnostics and contribute to informed maintenance decisions for the pumping unit.

INDEX TERMS AC motors, dynamometers, measurement techniques, oil drilling.

I. INTRODUCTION

Sucker Rod Pumping system (SRPS) is one of the primary methods of artificial oil lifting. This method is one of the artificial oil lifting methods most used around the world. Simplicity, reliability, and applicability for a wide range of operating conditions are advantages. Most oil wells adopt this exploration method worldwide [1].

Figure 1 shows a typical schematic of an SRPS. The system includes many components such as a prime mover, gearbox, and tubing. The oil of the well lifts to the surface using a piston pump in the bottom fixed to a rod having a come-and-go movement. In most installations, an electric motor runs at high speed. A mechanical system converts its rotational movement into the linear one.

The associate editor coordinating the review of this manuscript and approving it for publication was Amin Mahmoudi.

During the process of oil extraction, SRPS is subject to failures. The most common method for fault diagnostics uses a dynamometer card (DC). A DC shows the relation between the load and the rod displacement. The curve presents the work conditions of pumping units with reliability and simplicity [2].

Sensors measure both the displacement and the load on the rod. However, such sensors are invasive, expensive, and require mechanical adaptation. Moreover, any failure in these sensors contributes to errors on DC. This fact can compromise the analysis and diagnosis of problems in the well [3].

In this paper, we propose an assessment of the possibility of improving an estimator of DC based on the terminal quantities of the driving motor. The method uses a state observer whose inputs are values of instantaneous motor torque and speed from continuously sensing speed, voltage,

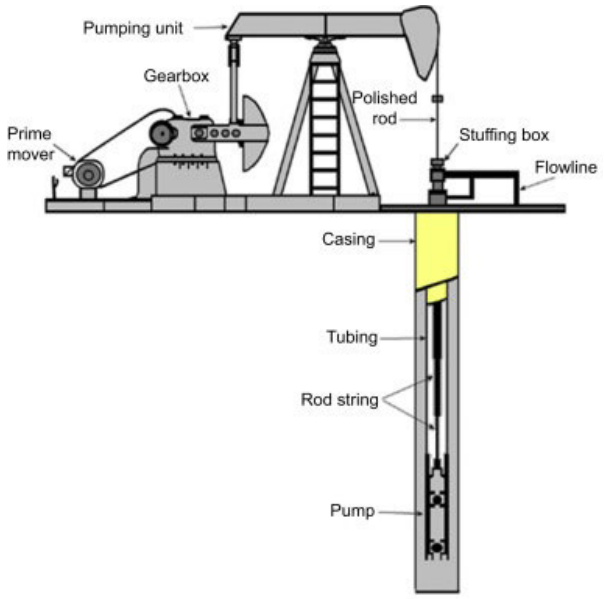

FIGURE 1. A schematic of a rod pumping system.

and current signals. Using geometry and the gearbox ratio of the rod pumping unit, the next step is computing the instantaneous position and load of the polished rod. The instantaneous operating parameters of the polished rod determine the surface dynamometer card. Experiments compare DC built from the method to show its efficiency.

The organization paper is as follows. The section I introduces the context and justification of the research. The section II brings the literature review. The section III describes the proposed method to obtain the DC. The section IV shows simulations and experimental results. The section V presents the conclusion of the research.

II. LITERATURE REVIEW

The main tool for diagnosing faults in SRPS is the DC. Obtaining this tool usually involves measuring the load and position of the polished rod. Instruments and sensors involved in this process are expensive, and any failure can compromise monitoring. With the increasing technological development, recent research pays attention to applying alternative methods.

The complexity of downhole conditions in SRPS difficulties fault diagnosis and prediction, a hot issue of concern for oilfield staff. Aiming at this problem, Sun [4] adopts the invariant moment theory to extract the eigenvalues of the dynamometer card, and uses the eigenvalues of the DC as the prediction variables of the model. However, the use of this model requires previously obtaining the DC.

Xiao et al. [2] proposed a learning-based framework for working conditions diagnosis of Oil well through dynamometer cards identification. An oil field served as the research source to investigate the properties of pumping systems under different working conditions and create a dataset.This study guided the design and implementation of learning-based oil well working conditions intelligent diagnosis system. The technique incurs a significant increase in computational cost due to the training of convolutional neural networks. Furthermore, training neural networks requires a large amount of data.

Asynchronous electric motors are usually used for the power supply of the SRPS. The rotating motion of its shaft transforms into a mechanical pumping movement. The effect of the static and dynamic loads exerted on the sucker rod string is also transmitted to these electric motors. Thus, it is possible to establish the relation between the electric motor and the force on the rod [1], [5].

Zuo et al. [1] proposed a hybrid model for indirect measurement DC based on measured motor power. From on the mechanical model analysis of SRPS, the dataset is constructed by transforming the motor power and geometric parameters of the SRPS into the polished rod torque, the first, and second derivatives of polished rod torque, and the torque factor. Despite experimental and prediction results, presenting about relative error below 3%, the proposed method requires a relevant computational cost, and considered only three single working conditions of SRPS.

To solve the need for external instruments for diagnostic rod pumping systems, Li et al. [3] established a practical parameter estimator for dynamometer card by measuring terminal data of drive motor. The method combined the T-type equivalent circuit model of induction motors and the model of beam pumping unit in order to acquire the surface dynamometer card in real time. However, the results calculated by the estimator can be improved to reduce the relative error when taking the experimental results as a reference.

In this paper, we present a groundbreaking model that revolutionizes the conventional approach to diagnostic rod pumping systems. Our model addresses the critical need to reduce reliance on external instruments for obtaining dynamometer cards, ultimately minimizing costs and significantly lowering the relative error when compared to experimental results. What sets our model apart is its incorporation of additional input variables into the estimator and a novel method for motor velocity acquisition. This innovation offers an alternative means of acquiring surface dynamometer cards, functioning as a complementary tool for fault diagnostics and facilitating well-informed maintenance decisions for the pumping unit.

III. METHOD DESCRIPTION

The dynamometer card (DC) captures load variations on the polished rod relative to its displacement within the pumping unit's cycle. Typically, creating a plot demands the installation of dynamometer equipment, consisting of force and position sensors, along with an algorithm to depict force against rod position. Alternatively, a plot can be generated by employing a motor torque signal and subsequently deriving the polished rod force. This approach proves useful due to the abundance of insights concerning rod pumping systems

concealed within the real-time power waveforms of the pumping unit motor [1], [3], [5].

Taking into account the contributions Gao et al. [3], we propose an enhancement to the estimation of the surface dynamometer card. While relying on the terminal quantities of the driving motor, this method introduces innovations in motor observer inputs as well as the acquisition of crank velocity and angle. Expanding the input variables of the motor observer and incorporating crank velocity measurements led to adjustments in the estimated dynamometer card plot, bringing it closer to reality. Figure 2 shows the block diagram of the system.

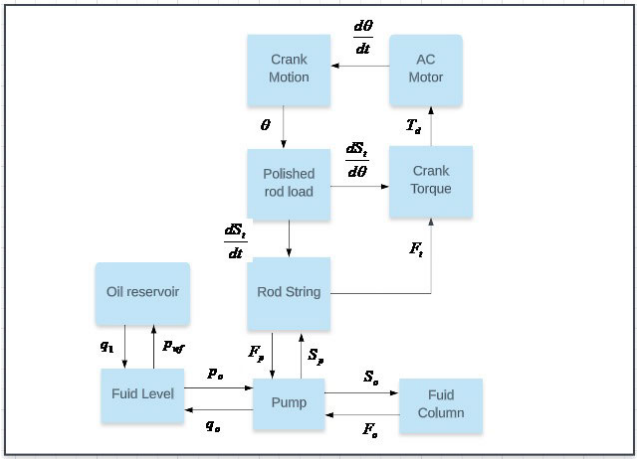

FIGURE 2. Block diagram of the coupled model (See [3]).

A. STRUCTURE OF PARAMETER ESTIMATOR

The method is executed utilizing measurements of motor electric currents, voltages, slip, and velocity as inputs. Real-time measurement of motor and crank velocity is facilitated through an optical tachometer. The synchronous motor speed aids in deducing slip. Motor electric current and voltage are gauged using a probe and a voltmeter, respectively.

The Motor Observer is a numerical algorithm developed within an interactive software designed for high-performance applications. Leveraging the T-type equivalent circuit model of the induction motor and utilizing input variables, it estimates the motor's torque.

Since the polished rod load estimator depends on both the crank angle and motor torque, it can be utilized to calculate the rod load. Consequently, by integrating these calculations with the pumping unit's geometry parameters and the angular displacement of the crank over time, it becomes possible to estimate a surface dynamometer card. Figure 3 shows a block diagram depicting the estimation method.

B. MODEL OF INDUCTION MOTOR

To describe the induction motor of the pumping unit, we employ the T-type equivalent circuit model [6] as depicted in Figure 4. Given that oil wells can be situated in remote locations, we have enhanced the T-type model by

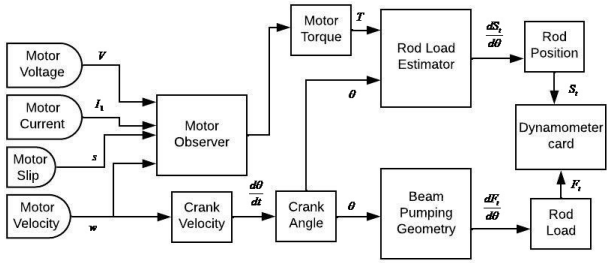

FIGURE 3. Estimation strategy.

incorporating additional elements, specifically R_S, R_L, and X_L, to account for supplementary losses arising from feeding line resistance and inductance, respectively.

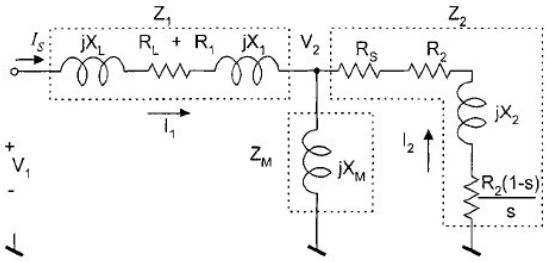

FIGURE 4. Model of induction motor.

The branch currents are given by

$$I_1 = V_1 \frac{1 + \frac{Z_2}{Z_M}}{Z_1 + Z_2 + \frac{Z_1 Z_2}{Z_M}}, \tag{1}$$

$$I_2 = \frac{V_1}{Z_1 + Z_2 + \frac{Z_1 Z_2}{Z_M}}, \tag{2}$$

where

$$Z_1 = R_1 + R_L + j(X_1 + X_L), \tag{3}$$

$$Z_2 = R_2 + R_S + \frac{R_2(1-s)}{s} + jX_2, \tag{4}$$

and

$$Z_M = jX_M. \tag{5}$$

Input complex power and output torque are

$$P_1 = V_1 I_1^* \tag{6}$$

$$T = \frac{P_2}{2\pi f_s} \tag{7}$$

The real power delivered to load is

$$P_2 = \frac{R_2(1-s)}{s} I_2^2 \tag{8}$$

where s is the slip, $f_0 = 60Hz$, and $f_s = f_0(1-s)$ is the rotator frequency.

C. PUMPING UNIT MODELLING

A sucker-rod pumping system comprises several key components, including a prime mover, gear reducer, pumping unit, sucker-rod string, and subsurface pump. Within this system, the pumping unit plays a pivotal role as it operates as a four-bar linkage mechanism, efficiently converting the rotary motion generated by the motor into a vertical motion applied to the polished rod.

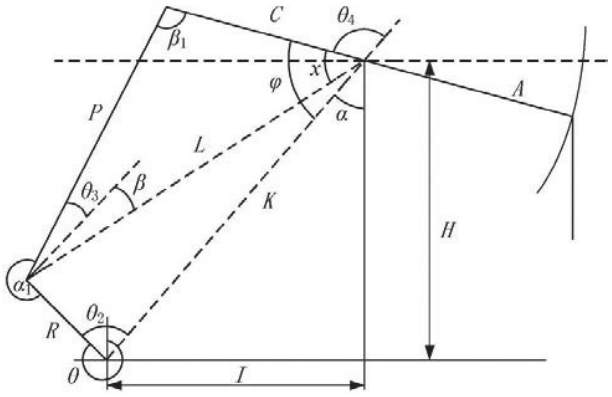

FIGURE 5. Four-bar linkage.

Figure 5 illustrates the simplified diagram of the pumping unit. Based on the geometric relationships depicted in the diagram, we can derive the following equations:

$$K = \sqrt{H^2 + I^2}, \tag{9}$$

$$L = \sqrt{R^2 + K^2 - 2KRcos(\theta_2)}, \tag{10}$$

$$\theta_2 = 2\pi - \theta + \alpha, \tag{11}$$

$$\alpha = \arcsin(1/K), \tag{12}$$

$$\chi = \arccos\left(\frac{C^2 + L^2 - P^2}{2CL}\right), \tag{13}$$

$$\phi = \chi + \beta, \tag{14}$$

$$\theta_3 = \arccos\left(\frac{P^2 + L^2 - C^2}{2PL} - \beta\right), \tag{15}$$

and

$$\theta_4 = \arccos\left(\frac{P^2 - L^2 - C^2}{2PL} - \beta\right). \tag{16}$$

Here, we define the following variables: R as the radius of the crank, P as the length of the pitman, C as the length of the backward beam, A as the length of the forward beam, K as the length of the fixed rod, L as the auxiliary line connecting the beam and the crank's radius, I as the horizontal height from the support point to the center of the gearbox,and H as the vertical height from the support point to the center of the gearbox.The geometry size of the pump jack is provided in Table 1.

The relationship between the polished rod position and the crank angle θ is as follows:

$$S(\theta) = \frac{A}{2}(1 - cos(\theta)). \tag{17}$$

TABLE 1. Geometry size of beam pumping unit.

Item	Value
A/mm	1800
C/mm	1440
P/mm	2010
H/mm	3174
I/mm	1380
L/mm	2472.59
K/mm	3461.02
R/mm	690
$\theta_0/^\circ$	0

D. POLISHED ROD LOAD MODELLING

Analysis during each pumping cycle shows that the polished rod experiences cyclic load profiles. Various methods, such as load cells and dynamometers, are employed for load measurement. These sensors are typically inserted into the top of the polished rod body. It's important to note that any failure in these components can disrupt oil production, necessitating pump unit maintenance.

In both modeling and indirect measurement (inference) of the polished rod load, relevant publications can be found in recent technical literature [1], [7], [8], [9]. In the context of mathematical modeling, a dynamic description of pumping dynamics that accounts for system inertia was proposed in [10], as follows:

$$\begin{aligned} T_R(\theta(t)) = \; & T_F(\theta(t))\Big(Q_{PR}(\theta(t)) - Q_{SU}\Big) \\ & -M\ sin\Big(\theta(t) + \tau\Big) - \Big(I_{M2}\,\dot{w}(t)\Big) \\ & + \left(\frac{T_F(\theta(t))\,I_{M3}}{A^2}\,\ddot{S}(t)\right) \end{aligned} \tag{18}$$

where

- $Q_{PR}(\theta(t))$: Polished rod load;
- $T_F(\theta(t))$: Dimensionless torque factor;
- M: Moment of counterbalance;
- Q_{SU}: Structural unbalance;
- τ: Phase angle (measured in radians, referencing the sinusoidal steady-state model);
- θ: Crank turning angle (measured in radians);
- I_{M2}: Inertia moment of spinning parts;
- I_{M3}: Inertia moment of articulated parts;
- $S(t)$: Polished rod position;
- $\omega(t)$: Crank angular speed (measured in radians per second);
- A: Walking beam.

This paper presents a method for continuous estimation of the polished rod load without relying on external devices such as load cells, strain gauges, or position transducers. In this process, crank angle and beam pumping geometry are fundamental. It's crucial to note that an electrical subsystem is coupled with a mechanical subsystem operating at different

timescales. The electrical system operates in a sinusoidal steady state, while the mechanical system involves factors like inertia and non-linearity in its components. These considerations impact the selection of sampling rates and bandwidths during signal processing to minimize errors in the estimation results.

The motor torque is coupled to the polished rod through a reducer unit, and this coupling can be modeled as follows:

$$T_M(\theta(t)) = EF_M EF_R \frac{1}{REL_{polleys}} \frac{1}{REL_R} Te, \tag{19}$$

and

$$REL_{polleys} = \frac{DP_R}{DP_M}, \tag{20}$$

where,

- EF_M: Motor efficiency;
- EF_R: Reducer efficiency;
- DP_R: Reducer pulley diameter;
- DP_M: Motor pulley diameter;
- REL_R: Reduction ratio.

As $\frac{REL_{polleys}\, REL_R}{EF_M EF_R} = cte$, so (19) can be rewritten as

$$T_M(\theta(t)) = \frac{1}{k_x}\, Te \tag{21}$$

where k_x is a constant.

Still, $w(t) = \dot{\theta}(t)$ then one can get

$$\ddot{S}(t) = \frac{\dot{S}(t)}{dt} = \frac{\dot{S}(t)}{d\theta}\frac{d\theta}{dt},$$
$$\ddot{S}(t) = \frac{d\left(\frac{dS(t)}{d\theta}\frac{d\theta}{dt}\right)}{d\theta}\frac{d\theta}{dt},$$

and

$$\ddot{S}(t) = [\ddot{\theta}(t)]^2 \frac{d^2S(t)}{d\theta^2} + \frac{dS(t)}{d\theta}\frac{dw(t)}{d\theta}\dot{\theta}(t).$$

So $\ddot{S}(t)$ can be rewritten as

$$\ddot{S}(t) = [\ddot{\theta}(t)]^2 \frac{d^2S(t)}{d\theta^2} + \frac{dS(t)}{d\theta}\dot{\theta}(t). \tag{22}$$

By substituting equations (21) and (22) into equation (18), we can derive a mathematical model for inferring the load on the polished rod as follows:

$$\begin{aligned} Q_{PR}(\theta(t)) = {} & \frac{1}{T_F(\theta(t))}\left(T_M(\theta(t))\, k_x + M\, sin(\theta(t)+\tau)\right) \\ & + Q_{SU} - \left[\frac{I_{M3}}{A^2}\frac{dS(t)}{d\theta} - \frac{I_{M2}}{T_F(\theta(t))}\right]\ddot{\theta}(t) \\ & - \frac{I_{M3}}{A^2}\left[w(t)\right]^2 \frac{d^2S(t)}{d\theta^2}. \end{aligned} \tag{23}$$

Assuming negligible values for I_{M2} and I_{M3}, equation (23) can be simplified to:

$$\begin{aligned} Q_{PR}(\theta(t)) = {} & \frac{1}{T_F(\theta(t))}\left(T_M(\theta(t))\, k_x + M\, sin(\theta(t)+\tau)\right) \\ & + Q_{SU}. \end{aligned} \tag{24}$$

IV. SIMULATION RESULTS

In the oil industry, operational oil wells are often inaccessible for academic research. Therefore, simulation models are employed within the structure illustrated in Figure 6. This structure represents the Artificial Elevation Laboratory (LEA) at the Federal University of Bahia (UFBA), Brazil. The LEA is designed to replicate conditions akin to those encountered in oil drilling and extraction operations. It serves as a valuable resource for scientific research and studies on oil elevation methods.

FIGURE 6. Photograph of the experimental setup.

The laboratory features three full-scale production wells dedicated to research purposes. The first well is equipped with a submerged centrifugal pumping system. The second well is equipped with a sucker rod pumping system, which is an experimental component of this research and has undergone testing and validation. The third well is equipped with submerged mechanical pumping of double effect. The proposed parameter estimation strategy was implemented within the LEA, simulating various operating conditions, including normal operation, gas interference, traveling valve leakage, and insufficient liquid supply.

The terminal characteristics of the induction motor, displacement, and the polished rod load are directly measured by the rod pumping data acquisition system, as depicted in Figure 7. Rotor velocity, denoted as $\frac{d\theta}{dt}$, is captured by an optical sensor. The AC Drive is responsible for motor speed control and simultaneously transmits motor control information, including AC voltage (V), stator current (I), and slip (s), to the PLC via the DeviceNet14 industrial network. The PLC, in turn, communicates with the OPC server using the TCP/IP protocol. Signals from the position transducer and load cell are transmitted to the PLC in standard 4-20mA.

We installed a position transducer and a load cell to generate the surface dynamometer card for evaluating the performance of the estimator in this study, as illustrated in Figure 8. This instrumentation assists in acquiring authentic dynamometer cards under various operational scenarios. We then compare these dynamometer

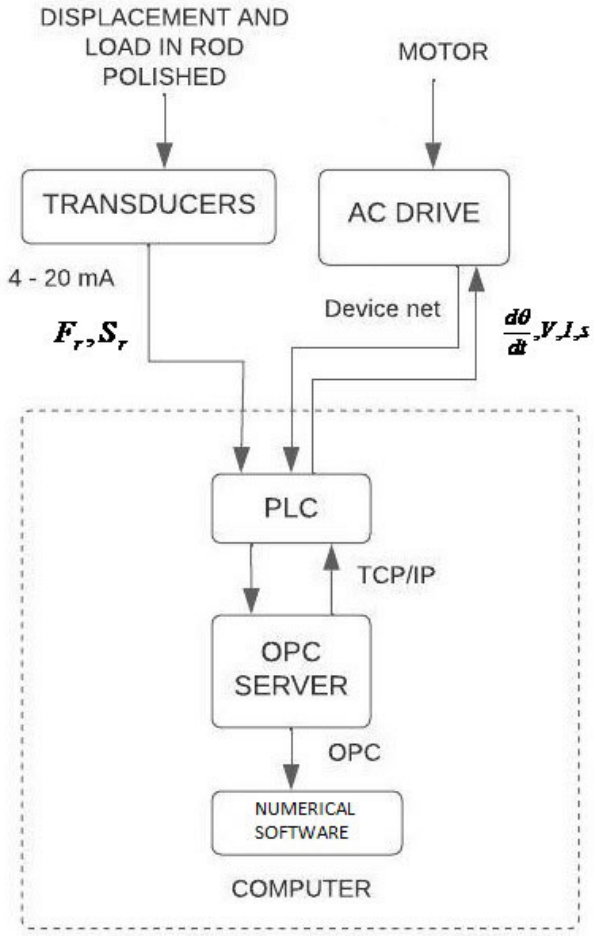

FIGURE 7. The hardware structure of rod pumping monitoring.

FIGURE 8. Detail of load cell and position transducer.

cards with those generated by the proposed model (See Figures 10, 11, 12 and 13).

The terminal quantities of the driving motor are measured using sensors such as dedicated probes and voltmeters. Mechanical structure data for the pumping station are obtained from the manufacturer's manual.Tables 2 and 3 display the specifications for the induction machine and the geometry data for the LEA pumping unit, respectively.

TABLE 2. Induction machine of pumping unit (LEA-UFBA).

Item	Specifications
Rated Frequency	60 Hz
Rated rpm	1160
Rated Power	3728.5 kW
Rated Current	8.86 A
Rated Voltage	380 V

TABLE 3. Features of the oil well artificial (LEA-UFBA).

Data	Measure(m)
Well depth	32
Well diameter	0.251
polished rod length	0.635
Diameter of the discharge piping	0.0588
Diameter of the piston actuator force	0.100
Diameter of the actuator stem strength	0.040
Diameter piston plunger pump	0.080
Diameter of the actuator rod pumping	0.040
Course of force actuators and pumping	1.5

Data from the motor is recorded in a file and processed alongside mechanical information. An algorithm developed within the numerical software manages all of this offline. It's important to recognize that this aspect presents a limitation that requires improvement, as real-time data acquisition tests have not been conducted as of yet.

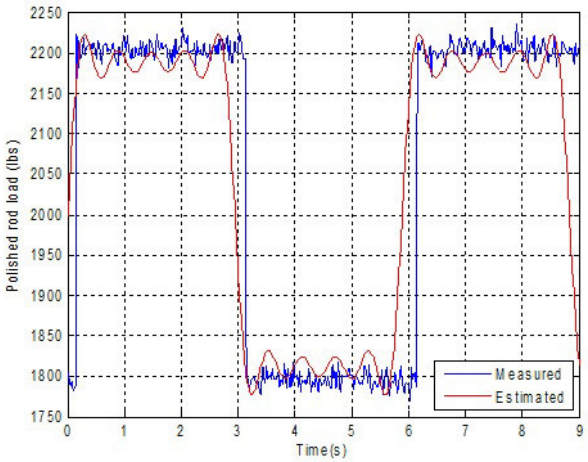

FIGURE 9. Comparing polished rod loads.

Figure 9 showcases the pumping unit operating at 10 cycles per minute. The conventional instrumentation records maximum and minimum polished rod load values of 2200 lbs and 1800 lbs, respectively. In contrast, the proposed method estimates maximum and minimum polished rod loads of approximately 2230 lbs and 1770 lbs, respectively. Two instances of relative equilibrium are identifiable, marking the

moments when the load on the polished rod stabilizes at its maximum and minimum values. These moments correspond to the times when the mechanical horsehead of the pumping unit reverses direction during the fluid extraction from the oil well.

With the estimator employed in this study, surface dynamometer cards were obtained in the experimental oil laboratory and subsequently compared to real dynamometer cards, as illustrated in Figures 10, 11, 12, and 13. Across all the results, the measured range for maximum and minimum polished rod loads has fluctuated within the approximate range of 3500 lbs to 450 lbs. The average values for the polished rod load, both estimated maximum and minimum, stand at 3200 lbs and 550 lbs, respectively.

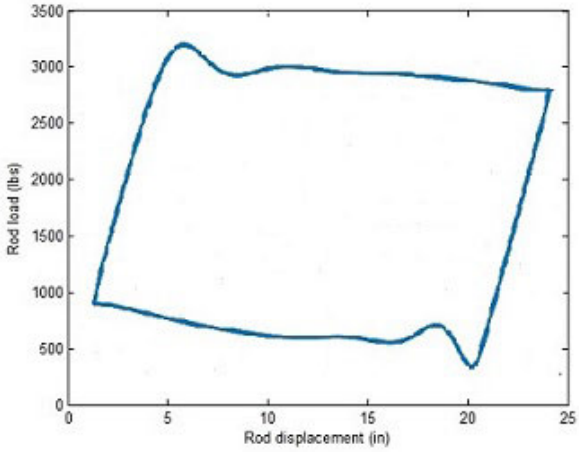

(a) Real Dynamometer Card

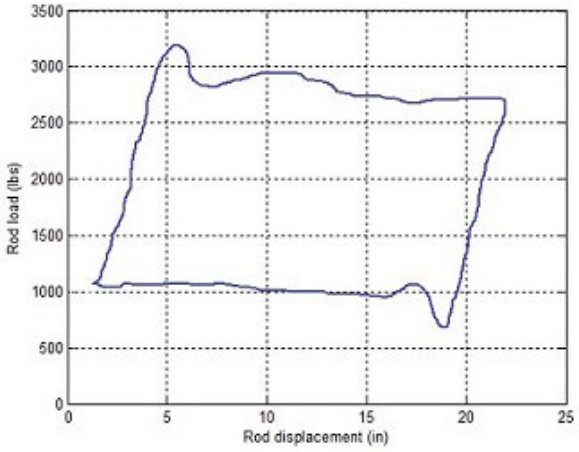

(b) Estimated Dynamometer Card

FIGURE 10. Normal working state.

In Figure 10, the results are displayed following the experimental laboratory (LEA) simulation designed to replicate the typical operation of an oil well. The measured and estimated maximum values for polished rod loads are approximately 3280 lbs and 3250 lbs, respectively. Regarding the measured and estimated minimum values for polished rod loads, these are 450 lbs and 550 lbs, respectively. In the statistical analysis, a total of 3600 data points are employed. The mean value is 1915.20 lbs, with a variance of 20.52 lbs. The percent relative error in the measured values is 0.92%, while in the estimated value, it is 2.22%. The 1.3% difference between the measured and estimated percentage relative errors suggests promising results for this particular condition of the oil well under study.

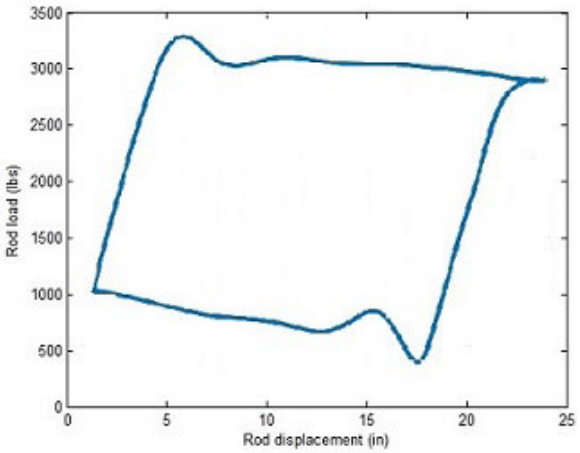

(a) Real Dynamometer Card

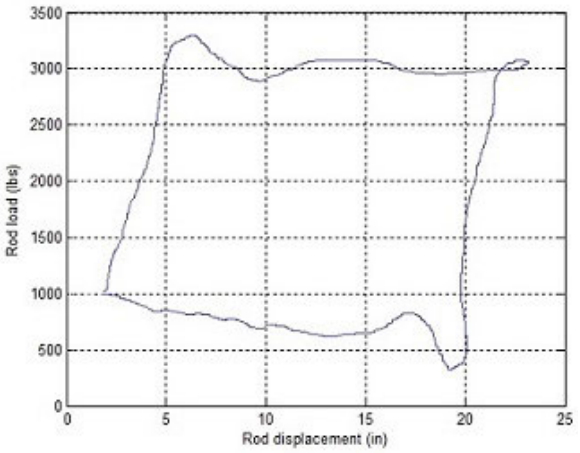

(b) Estimated Dynamometer Card

FIGURE 11. Gas affected.

In Figure 11, the experimental laboratory is configured to simulate gas affected. The relative errors, both measured and estimated, for the maximum and minimum values are 1.54% and 4.08%, respectively. This is due to the measured and estimated maximum polished rod loads being approximately 3250 lbs and 3300 lbs. In the statistical analysis, 3600 data points are employed. The mean value for polished rod loads is 1825.72 lbs, with a variance of 10.15 lbs. The measured and estimated minimum polished rod loads are 490 lbs and 470 lbs, respectively. Although the estimator yields satisfactory results for this operational state, it's essential to acknowledge the minimal difference between the outcomes under normal working conditions and the gas-affected state. Further investigations into the operation of the pumping unit in this state are warranted.

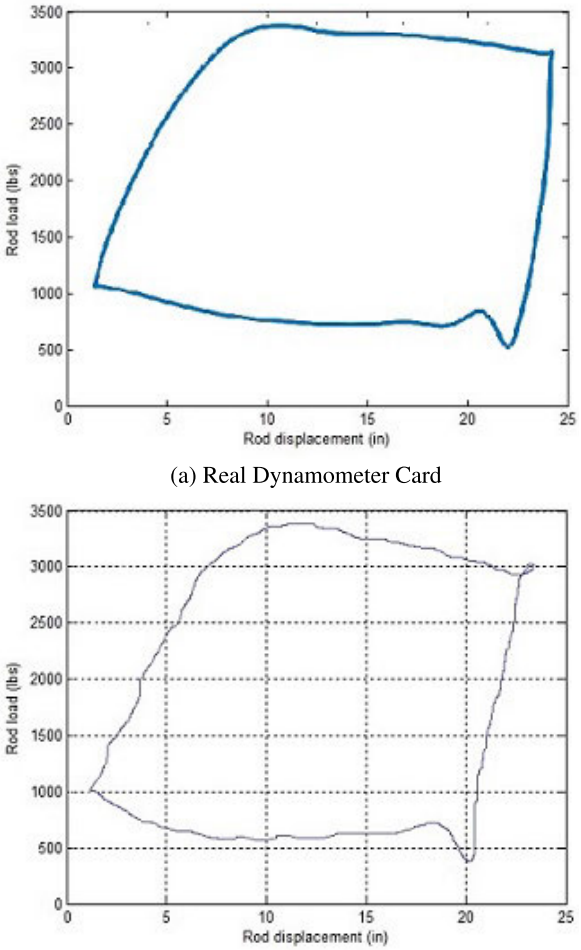

(a) Real Dynamometer Card

(b) Estimated Dynamometer Card

FIGURE 12. Travelling valve leakage.

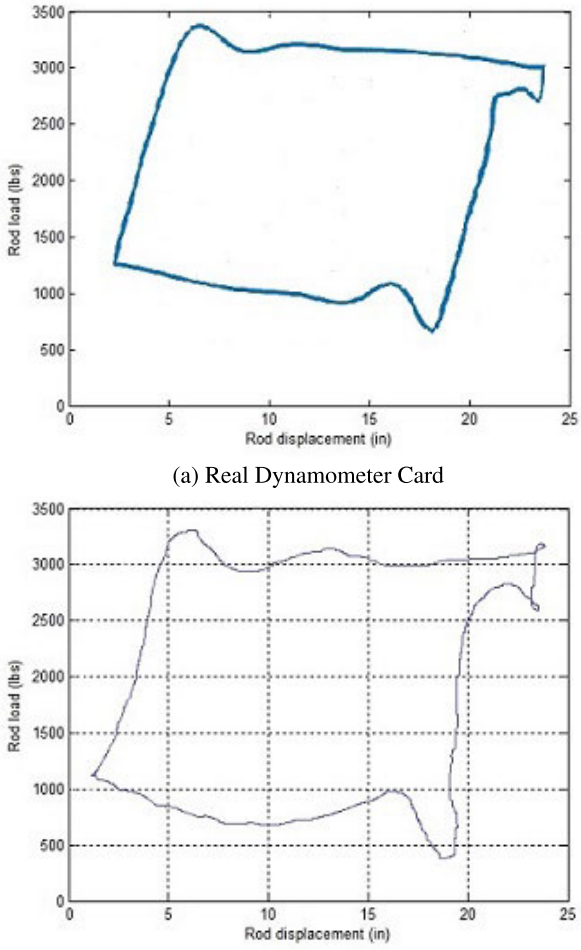

(a) Real Dynamometer Card

(b) Estimated Dynamometer Card

FIGURE 13. Insufficient liquid supply.

In Figure 12, the experimental laboratory is configured to simulate travelling valve leakage. The measured and estimated maximum polished rod loads are approximately 3400 lbs and 3380 lbs, while the measured and estimated minimum loads for the polished rod are 500 lbs and 470 lbs. For the statistical analysis, a dataset of 3600 points is employed. The mean value of the polished rod loads is 1895.87 lbs, and the variance is 9.72 lbs. The relative errors for the measured and estimated values are 0.59% and 6%, respectively. The difference between the measured and estimated percent relative errors is in the order of 5.5%. This indicates relevant degree of precision in the results.

Figure 13 displays the results of the experimental laboratory configured to simulate insufficient liquid supply. The measured and estimated maximum polished rod loads are 3400 lbs and 3250 lbs, respectively, while the measured and estimated minimum polished rod loads are 500 lbs and 470 lbs, respectively. For the statistical analysis, a dataset of 3600 points is employed. The mean value for polished rod loads is 1935.59 lbs, with a variance of 13.12 lbs. The relative errors for the measured and estimated values are 4.41% and 6%, respectively. The difference between the measured and estimated percent relative errors is in the order of 1.59%. This demonstrates a significant level of precision in the results compared to the simulation of traveling valve leakage.

Based on a comprehensive analysis of the values obtained from the proposed estimator presented in Figures 10, 11, 12, and 13, the results tend to align with the measured
results.

Gao et al. [3] introduced an estimator with two input parameters, namely motor voltage and current. Speed and torque were then estimated based on the T-type model of the motor equivalent circuit. These electrical inputs, coupled with details about the mechanical configuration of the pumping unit, were used to generate the dynamometer card. In our proposal, we aim to modify this framework by incorporating additional input parameters. In addition to voltage and current, we introduce slip and the directly measured speed of the motor. The algorithm we've developed is specifically designed to estimate torque, and when combined with data

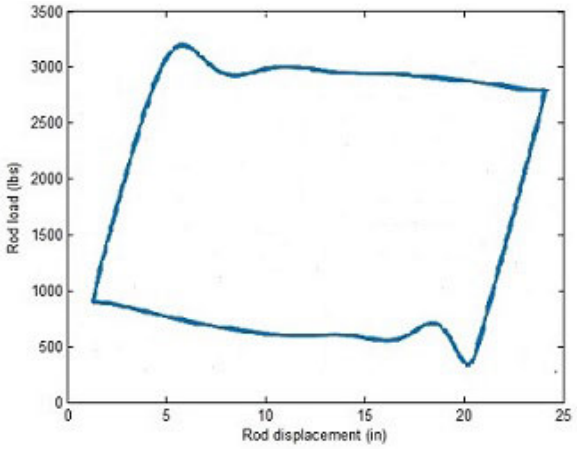

(a) Real Dynamometer Card

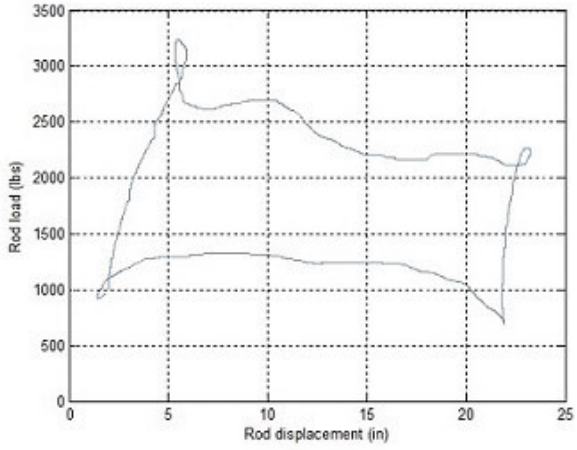

(b) Estimated Dynamometer Card with the proposed method by [3]

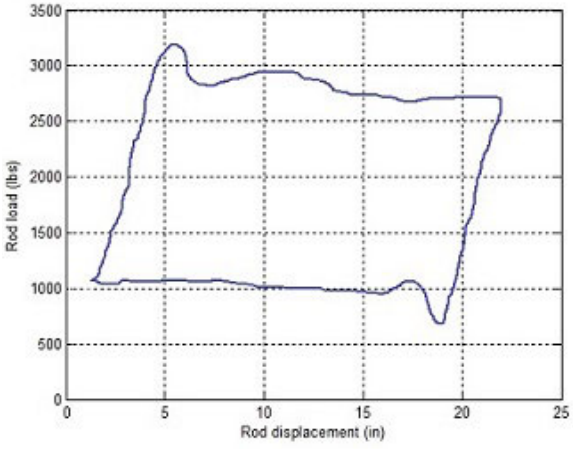

(c) Estimated Dynamometer Card with our method

FIGURE 14. Normal working state.

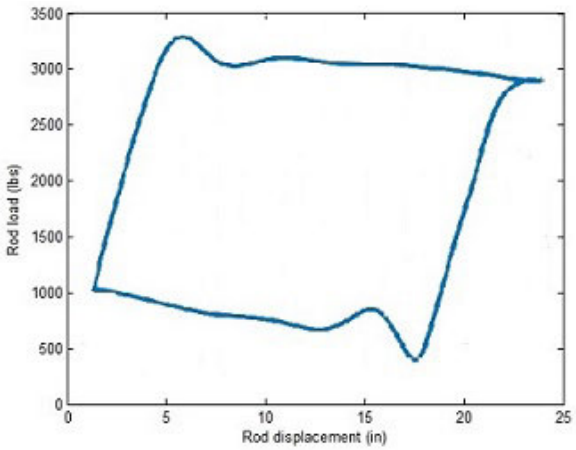

(a) Real Dynamometer Card

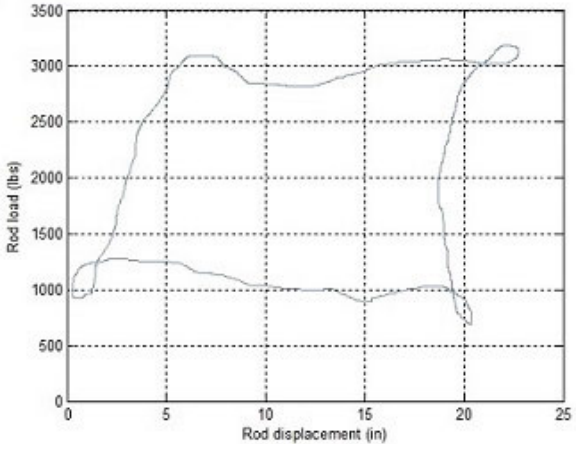

(b) Estimated Dynamometer Card with the proposed method by [3]

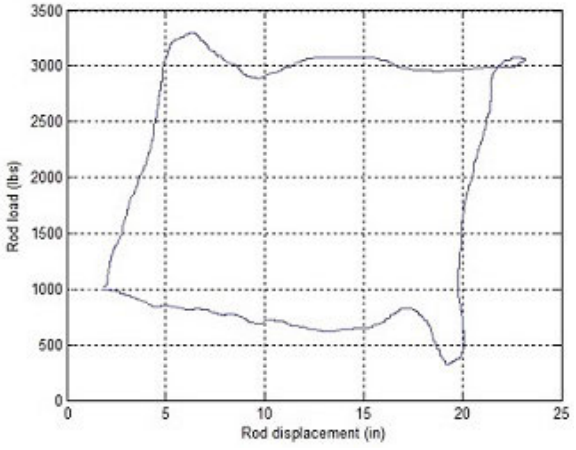

(c) Estimated Dynamometer Card with our method

FIGURE 15. Gas affected.

regarding the mechanical structure of the pumping unit, it enables the generation of the dynamometer card.

Figures 14, 15, 16, and 17 depict the comparisons between the outcomes of the method introduced in this study and the one proposed by Gao et al. [3] for estimating the dynamometer card. Across all the figures, the utilization of our method indicates a greater approximation of the curves when compared to their respective real counterparts, despite our method requiring more measure from the terminal quantities of the driving motor.

In Figure 14, when both methods are tested using the experimental laboratory simulating normal operation, the

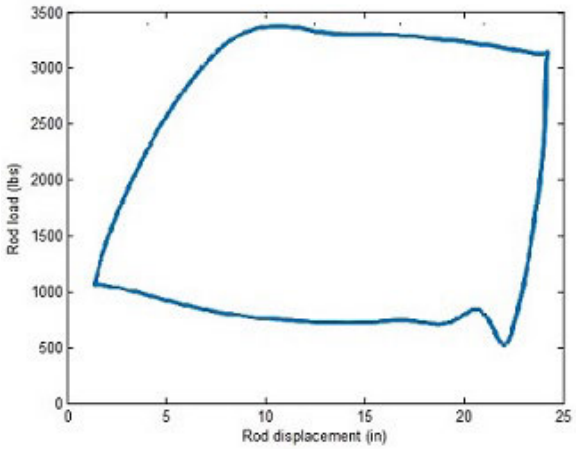

(a) Real Dynamometer Card

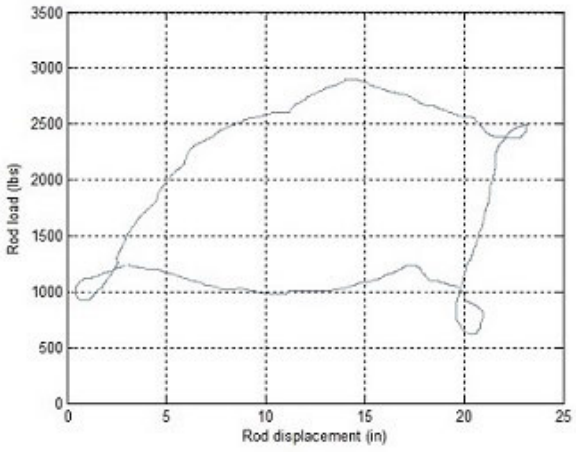

(b) Estimated Dynamometer Card with the method proposed by [3]

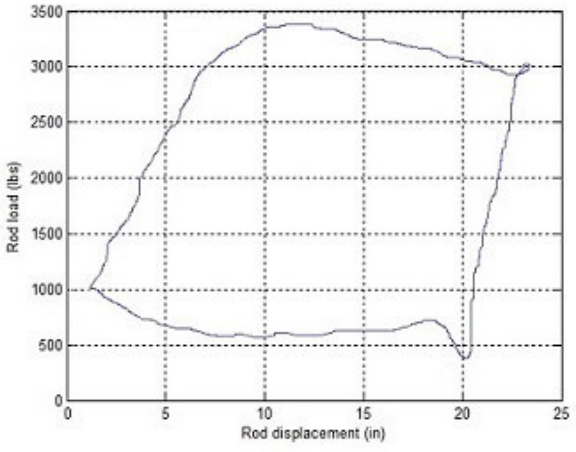

(c) Estimated Dynamometer Card with our method

FIGURE 16. Travelling valve leakage.

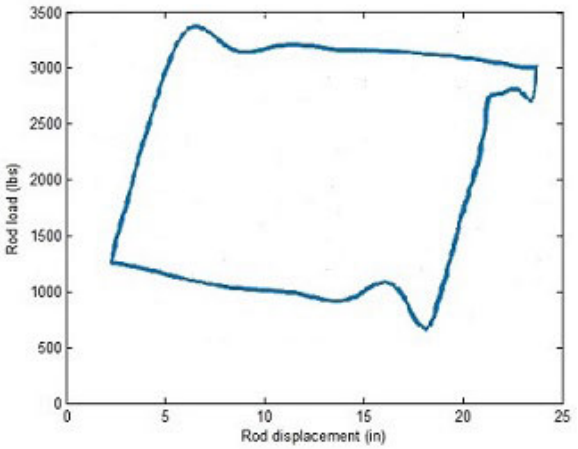

(a) Real Dynamometer Card

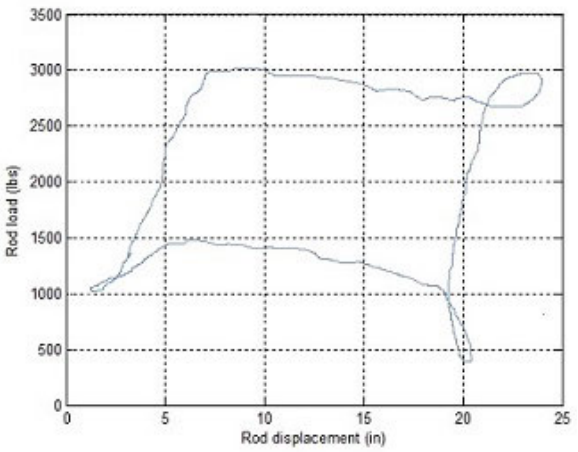

(b) Estimated Dynamometer Card with the method proposed by [3]

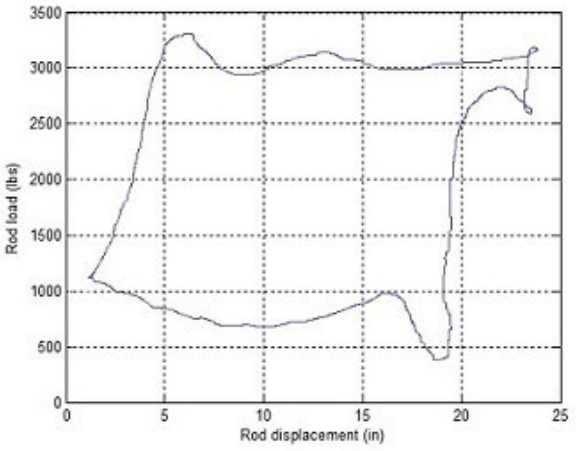

(c) Estimated Dynamometer Card with our method

FIGURE 17. Insufficient liquid supply.

estimated maximum polished rod loads are approximately 3380 lbs and 2980 lbs, while the estimated minimum polished rod loads are around 450 lbs and 650 lbs. In the statistical analysis involving 3600 data points, a comparison is made between the curve obtained by the method proposed by Gao et al. [3] and the respective real curve (see Figure 10). For the Gao et al. [3] method, the mean value is 1979.52 lbs, the variance is 78.23 lbs, and the relative error between the measured and estimated values was 2.72%. In contrast, when the method proposed in this work is applied, the mean value is 1915 lbs, the variance is 20.52 lbs, and the relative error

for the estimated values was 2.22%. This represents a 0.5% enhancement in the precision of the results.

In Figure 15, the estimated maximum polished rod loads are approximately 3300 lbs and 3180 lbs, while the estimated minimum polished rod loads are around 470 lbs and 680 lbs. In the statistical analysis involving 3600 data points, a comparison is made between the curve obtained by the method proposed by Gao et al. [3] and the respective real curve (see Figure 11). For the Gao et al. [3] method, the mean value is 1875.32 lbs, the variance is 50.72 lbs, and the relative error between the measured and estimated values is 7.92%. However, when the method proposed in this work was applied, the mean value is 1825.72 lbs, the variance is 10.15 lbs, and the relative error for the estimated values is 4.08%. For this specific operational condition of the pumping unit, further studies are warranted, as the relative errors are more significant when compared to other operating conditions that have been investigated.

In Figure 16, the estimated maximum polished rod loads are approximately 3380 lbs and 2980 lbs, while the estimated minimum polished rod loads are about 470 lbs and 620 lbs. In the statistical analysis involving 3600 data points, a comparison was conducted between the curve obtained using the method proposed by Gao et al. [3] and the respective real curve (see Figure 12). For the Gao et al. [3] method, the mean value was 1773.82 lbs, the variance was 35.09 lbs, and the relative error between the measured and estimated values was 3.22%. Conversely, when the method suggested in this work was applied, the mean value was 1895.87 lbs, the variance was 9.72 lbs, and the relative error for the estimated values was 1.62%.

TABLE 4. Comparative table of the methods.

Simulation Condition	Reference Method Relative error (%)	Our Method Relative error (%)
Normal Working State	2.72	2.22
Gas Affected	7.92	4.08
Travelling Valve Leakage	3.22	1.62
Insufficient Liquid Supply	4.84	2.61

In Figure 17, the estimated maximum polished rod loads are approximately 3250 lbs and 3220 lbs, with estimated minimum loads of around 470 lbs and 610 lbs. In the statistical analysis, which involved 3600 data points, we compared the curve generated using the method proposed by Gao et al. [3] with the corresponding real curve (see Figure 13). Using the Gao et al. [3] method, we obtained a mean value of 1895.72 lbs, a variance of 39.53 lbs, and a relative error between the measured and estimated values of 4.84%. Conversely, when applying the method proposed in this work, we achieved a mean value of 1935.59 lbs, a variance of 13.12 lbs, and a relative error for the estimated values of 2.61%.

Table 4 provides a summary of the comparison between the two methods under investigation. The results from the tests, comparing the two investigated methods under conditions of traveling valve leakage and insufficient liquid supply, indicate enhancements in precision. However, there is room for further improvement in refining the contours of the dynamometer card curves estimated through the method proposed in this work. Additionally, the optimization of measures related to dispersion, mean value, and relative error can be achieved by conducting a more comprehensive examination and enhancement of the developed algorithm.

V. CONCLUSION

This paper establishes a correlation between the surface dynamometer card and the terminal characteristics of the AC induction motor in rod pumping systems. To acquire the properties of rod pumping systems under four distinct laboratory-simulated scenarios, this paper introduces a functional parameter estimator. This estimator combines an equivalent circuit model of induction motors with a model of the beam pumping unit to obtain the surface dynamometer card through the measurement of the AC motor's terminal parameters.

The novelty of this approach lies in the expansion of the estimator's input variables and the direct measurement of motor velocity. While it necessitates additional measurements from the terminal quantities of the driving motor, these adjustments yield substantial enhancements in result accuracy. Although we conducted tests under four different operational scenarios of the pumping unit, particular emphasis should be placed on the investigation of the gas-affected state. Moreover, it is imperative to validate the effectiveness of the proposed method through real-world testing in an operational well, where real-time acquisition of AC motor terminal parameters can be implemented.

Despite this need, the overarching findings from the statistical analyses underscore the robust performance of the proposed method. The simulations demonstrate that the adopted methodology has the potential to contribute to the monitoring of rod pumping systems and to enhance the diagnosis of their operational conditions.

REFERENCES

[1] J. Zuo, Y. Wu, Z. Wang, and S. Dong, "A novel hybrid method for indirect measurement dynamometer card using measured motor power in sucker rod pumping system," *IEEE Sensors J.*, vol. 22, no. 14, pp. 13971–13980, Jul. 2022.

[2] R. Ma, H. Tian, X. Cheng, Y. Xiao, Q. Xu, and X. Yu, "Oil-net: A learning-based framework for working conditions diagnosis of oil well through dynamometer cards identification," *IEEE Sensors J.*, vol. 23, no. 13, pp. 14406–14417, Jul. 2023.

[3] X. Li, X. Gao, C. Yuan, Y. Hou, and X. Chen, "Practical parameter estimator for dynamometer card of rod pumping systems by measuring terminal data of drive motor," in *Proc. Chin. Control Decis. Conf. (CCDC)*. Nanchang, China: IEEE, Jun. 2019, pp. 4074–4077.

[4] W. Sun, W. Gao, W. Zhang, and T. Ren, "Study on working condition prediction of suck rod pumping system based on long short-term memory network," in *Proc. 5th Int. Conf. Intell. Control, Meas. Signal Process. (ICMSP)*, Chengdu, China, May 2023, pp. 1–4.
[5] E. R. Enikeeva and N. N. Alaeva, "Analysis of operation and ways to improve the efficiency of the pumping unit," in *Proc. Int. Conf. Ind. Eng., Appl. Manuf. (ICIEAM)*, Sochi, Russia, May 2023, pp. 1–5.
[6] H. Chen and C. Bi, "Optimal starting frequency of three-phase induction motor," *IET Electric Power Appl.*, vol. 16, no. 3, pp. 362–369, Mar. 2022.
[7] S. I. Tecle and A. Ziuzev, "A review on sucker rod pump monitoring and diagnostic system," in *Proc. IEEE Russian Workshop Power Eng. Autom. Metall. Ind., Res. Pract. (PEAMI)*, Magnitogorsk, Russia, Oct. 2019, pp. 85–88.
[8] K. Wang, G. Gong, R. Shen, A. Wang, Z. Yao, W. Mao, and H. Lu, "Novel physical network algorithm for indirect measurement of polished rod load of beam-pumping unit," *J. Eng.*, vol. 10, pp. 792–7287, May 2019.
[9] D. S. Torgaeva, N. A. Shalyapina, and M. P. Sukhorukov, "Simulation of load on a polished rod of sucker rod pump for oil production," in *Proc. Int. Multi-Conf. Eng., Comput. Inf. Sci. (SIBIRCON)*, Novosibirsk, Russia, Oct. 2019, pp. 0504–0508.
[10] S. G. Gibbs, "Computing gearbox torque and motor loading for beam pumping units with consideration of inertia effects," *J. Petroleum Technol.*, vol. 27, no. 9, pp. 1153–1159, Sep. 1975.

LÁZARO EDMILSON BRITO SILVA was born in Salvador, Brazil. He received the bachelor's degree in electrical engineering from the Federal University of Paraíba (UFPB), Campina Grande, Brazil, in 1998, and the master's degree in computational modeling from SENAI-CIMATEC, Salvador, in 2013. He has been a Professor with the Department of Education, Federal Institute of Bahia, since 2014. His current research interests include assistive technology, renewable energy, control systems, inference for monitoring systems, and signal processing for measuring purposes.

JÉS JESUS FIAIS CERQUEIRA (Member, IEEE) was born in Salvador, Brazil. He received the B.S. degree in electrical engineering from the Federal University of Bahia (UFBA), in 1992, and the M.Eng. and the Dr.Eng. degrees in electrical engineering from the School of Electrical and Computer Engineering, State University of Campinas (UNICAMP), Campinas, Brazil, in 1996 and 2001, respectively. Since 2000, he has been with the Department of Electrical and Computer Engineering, UFBA, and in 2017, he became a Full Professor. He was an Associate Editor of the *Journal of Control, Automation, and Electrical Systems* and he has been working with *Robotic Systems*, *Human-Robot Interaction*, *Computational Intelligence*, *Sensors and Actuators*, and *Nonlinear Systems*.

AMAURI OLIVEIRA (Life Senior Member, IEEE) was born in Rui Barbosa, Brazil, in 1954. He received the bachelor's degree in electrical engineering from the Federal University of Bahia (UFBA), Salvador, Brazil, in 1979, the master's degree in electrical engineering from the Federal University of Rio de Janeiro, Rio de Janeiro, Brazil, in 1982, and the Ph.D. degree in electrical engineering from the Federal University of Paraíba, Campina Grande, Brazil, in 1997. He was a Full Professor with the Department of Electrical and Computer Engineering, UFBA, from 1983 to 2018. His current research interests include electronic instrumentation, in particular, measurements systems, thermo-sensors, and signal processing for measuring purposes.

ANTONIO MARCUS N. LIMA (Senior Member, IEEE) was born in Recife, Pernambuco, Brazil, in 1958. He received the B.Eng. and M.Eng. degrees in electrical engineering from Universidade Federal da Paraıba (UFPB), in 1982 and 1985, respectively, and the Ph.D. degree in electrical engineering from Institut National Polytechnique de Toulouse, in 1989. He was with Escola Técnica Redentorista, from 1977 to 1982. He was a Design Engineer with Sul-América Philips, from 1982 to 1983. From March 1983 to March 2002, he was with the Department of Electrical Engineering (DEE), UFPB, where he became a Full Professor, in 1996. At UFPB, he was a Coordinator of Graduate Studies, from 1991 to 1993 and from 1997 to 2002. Since April 2002, he has been with the DEE, Universidade Federal de Campina Grande (UFCG), where he is currently a Full Professor. He was the Head of the DEE, UFCG, from 2002 to 2010. In 2010, he was admitted to the National Order of Scientific Merit in the category of Commander. Since 2014, he has been a Full Member of the Brazilian Academy of Sciences and the National Academy of Engineering. His current research interests include power electronics, automatic control, and biomedical engineering.